

Parameterizing the Distance Distribution of Undirected Networks

Christian Bauckhage

Fraunhofer IAIS and University of Bonn, Germany
 {fn.in}@iais.fraunhofer.de

Kristian Kersting and Fabian Hadiji

TU Dortmund University, Germany
 {fn.in}@cs.tu-dortmund.de

Abstract

Network statistics such as node degree distributions, average path lengths, diameters, or clustering coefficients are widely used to characterize networks. One statistic that received considerable attention is the distance distribution — the number of pairs of nodes for each shortest-path distance — in undirected networks. It captures important properties of the network, reflecting on the dynamics of network spreading processes, and incorporates parameters such as node centrality and (effective) diameter. So far, however, no parameterization of the distance distribution is known that applies to a large class of networks. Here we develop such a closed-form distribution by applying maximum entropy arguments to derive a general, physically plausible model of path length histograms. Based on the model, we then establish the generalized Gamma as a three-parameter distribution for shortest-path distance in strongly-connected, undirected networks. Extensive experiments corroborate our theoretical results, which thus provide new approaches to network analysis.

1 INTRODUCTION

As networks are combinatorial structures, network analysis typically relies on statistics such as node degree distributions, average path lengths, clustering coefficients, or measures of assortativity [11]. One statistic that received considerable attention is the distance distribution — the number of pairs of nodes for each shortest-path distance — in undirected networks. First of all, features such as average path lengths or network diameters can be determined therefrom. Second of all, path length statistics are closely related to velocities or durations of network spreading processes. Analytically tractable models of shortest path distributions would thus allow for inferring network properties as well

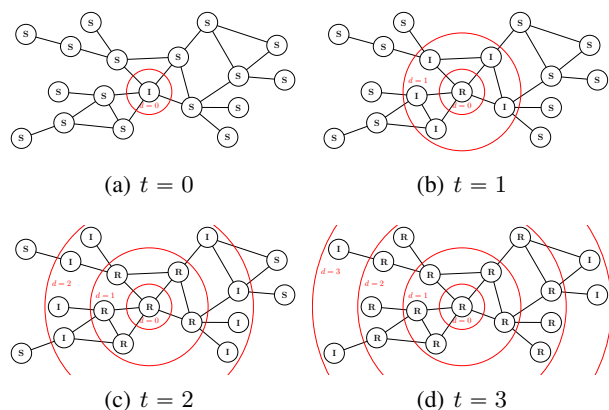


Figure 1: A highly infectious *SIR* cascade on a network realizes a node discovery process. (a) at onset time $t = 0$, most nodes are *susceptible* and only a single node is *infected*. (b)–(d) infected nodes immediately *recover* but always infect their susceptible neighbors. This way, the number of newly infected nodes n_t at time t corresponds to the number n_d of nodes that are at distance $d = t$ from the source node of the epidemic.

as for reasoning about diffusion dynamics. Yet, analytic models and in particular parameterizing the distance distribution prove difficult to achieve and related reports are curiously scarce [7, 9, 14, 34, 35]. Here, we contribute to these efforts and derive a novel, principled general model of shortest path length distributions in strongly connected networks. Considering a duality between network spreading processes and shortest path lengths, we then show that maximum entropy arguments as to diffusion dynamics lead to the generalized Gamma distribution as a three-parameter distribution in closed form.

The work presented here was motivated by questions as to the dynamics of network spreading processes. Models of such processes play an important role in various disciplines. They model the dynamics of epidemic diseases [20, 27, 22], explain the diffusion of innovations or viral messages [1, 24], and, in the wake of social media, a

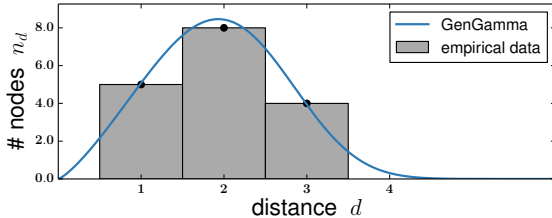


Figure 2: Shortest path histogram resulting from the network spreading process in Fig. 1 and a corresponding maximum likelihood fit of the generalized Gamma distribution.

quickly growing body of research develops graph diffusion models to study patterns of information dissemination in Web-based social networks [2, 10, 16, 25, 36]. Each of these examples concerns an instance of a rather general phenomenon: An agent (a virus, a rumor, an urge to buy a product, etc.) spreads in form of a contact process and thus cascades through a network of interlinked entities (people, computers, blogs, etc.). At the onset of the agent’s activity, many networked entities are *susceptible* to its effects but only few are actually *infected* (see Fig. 1(a)). As time progresses, susceptible entities related to infected ones may become infected whereas infected entities may remain infected, *recover*, become susceptible again, or even be removed from the population (see Fig. 1(b)–(d)). Crucial properties of such a process are its infection rate, its recovery rate, or the number of infected entities per unit of time. If an (information) epidemic is observed to rage through a community, these features help assessing its progression or final outbreak size and thus inform contagion or dissemination strategies. For instance, while public health authorities need to devise immunization protocols to curtail epidemic diseases, viral marketers typically aim at maximizing the effects of their campaigns. In any case, knowledge as to the structure of a community through which an epidemic spreads would be beneficial. Alas, in practice, community structures are hardly ever known but available information only consists of outbreak data as shown in Fig. 2.

Relating such outbreak data to network structures is the key idea underlying our contribution and is orthogonal to related approaches such as [2, 21, 26, 15, 36], which assume outbreak data *and* information about network members to be available and apply machine learning to identify hubs, link structures, or infection routes. Instead, we follow the paradigm in [4, 7, 16, 28, 29, 35] which asks for physical explanations of the noticeably skewed appearance of outbreak histograms and attempts to relate corresponding physical models to network properties.

More precisely, we make two technical contributions. First, we relate outbreak data to network structures via a novel maximum entropy model. Then, based on the model, we establish the generalized Gamma distribution as a physically-

plausible, continuous parameterization of the distance distribution of networks of arbitrary topology. Considering the fact that temporal distributions of infection counts in highly infectious spreading processes and distributions of shortest path lengths are dual phenomena allows us to invoke maximum entropy arguments from which we derive physical characterizations of path lengths- and outbreak statistics. In other words, our model results from first principles rather than from data mining. It also generalizes previous theoretical results [7, 35] and provides an explanation for a recent empirical observation as to path length distributions in social networks [8].

We proceed as follows. We start off by briefly reviewing existing analytical models of shortest path- and outbreak distributions in Section 2. Afterwards, we show that the generalized Gamma distribution naturally generalizes these, and discuss its properties and characteristics in Section 3. In particular, we demonstrate how the generalized Gamma emerges as a maximum entropy model of path length- and outbreak data. Before concluding, we support our theoretical results by exhaustive experiments on both synthetic and real-world graphs in Section 4.

2 KNOWN RESULTS

Analytically tractable models of shortest path length distributions and outbreak data are of considerable interest in the study of epidemic processes on networks. However, as networks are combinatorial structures, corresponding results are necessarily statistical [4, 7, 16, 28, 29, 35]. In a landmark paper [35], Vazquez studied the dynamics of epidemic processes in power law networks. Arguing based on branching process models, he showed that for networks whose node degree distribution has a power law exponent $2 < \gamma < 3$, the number of infected nodes at time t follows a *Gamma distribution*.

$$f_{GA}(t; \theta, \eta) = \frac{1}{\theta^\eta} \frac{1}{\Gamma(\eta)} t^{\eta-1} e^{-t/\theta} \quad (1)$$

where $\Gamma(\cdot)$ is the gamma function and $\theta > 0$ and $\eta > 0$ are scale and shape parameters, respectively. Curiously, for power law exponents $\gamma \geq 3$, this result does not apply. Concerned with Erdős-Rényi graphs, Bauchhage *et al.* [7] derived a different result. Based on models of the expected number of paths of length t between arbitrary nodes [9, 14], they resorted to extreme value theory [13] to show that infection counts can be characterized by the *Weibull distribution*.

$$f_{WB}(t; \lambda, \kappa) = \frac{\kappa}{\lambda^\kappa} t^{\kappa-1} e^{-(t/\lambda)^\kappa} \quad (2)$$

where $\lambda > 0$ and $\kappa > 0$ are scale and shape parameters. Neither model was obtained from mere empirical observations. Both follow from basic principles, provide *physically and hence socially plausible* and comprehensible characterizations of shortest path length distributions and diffusion dynamics, and were verified empirically.

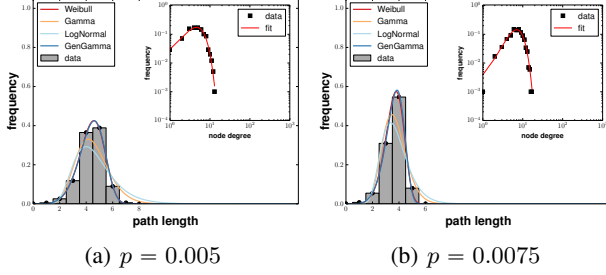


Figure 3: Qualitative examples of shortest path distribution in Erdős-Rényi graphs. Confirming [7], Weibull fits well. Yet, generalized Gamma provides better fits.

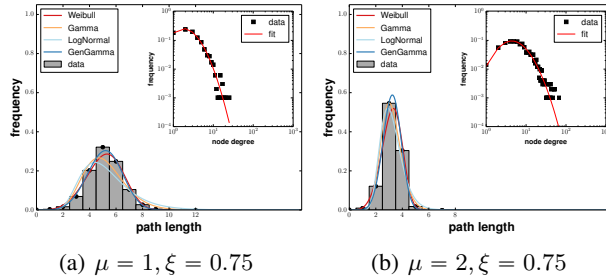


Figure 4: Qualitative examples of shortest path distribution in LogNormal graphs. For different node degree distributions, the models considered here provide more or less accurate fits. The generalized Gamma, however, always fits best (cf. Tab. 1).

Finally, Bild *et al.* [8] recently investigated information cascades and retweet networks on twitter and found that they could accurately fit their data using the *LogNormal distribution*

$$f_{LN}(t; \mu, \xi) = \frac{1}{\sqrt{2\pi} \xi t} e^{-\frac{(\log t - \mu)^2}{2\xi^2}} \quad (3)$$

where μ and ξ are location and scale parameters. Regarding our approach in this paper, we emphasize that (3) was not found theoretically but emerged empirically. At the same time, we note that the Gamma, Weibull, and LogNormal distribution may easily confused for one another [31]. Our discussion so far therefore begs the question if the above results are contradictory or if they can be unified within a more general framework? In the following, we will show that the latter is indeed the case.

3 A THREE-PARAMETER DISTANCE DISTRIBUTION

We will now establish the *generalized Gamma distribution* as a comprehensive model of the shortest path distributions and outbreak data in connected networks of arbitrary topology. Different versions of the generalized Gamma dis-

tribution can be traced back to 1920s [12]. Here, we are concerned with the three-parameter version that was introduced by Stacy [33]. Its probability density function is defined for $t \in [0, \infty)$ and given by

$$f_{GG}(t | \sigma, \alpha, \beta) = \frac{\beta}{\sigma^\alpha} \frac{1}{\Gamma(\alpha/\beta)} t^{\alpha-1} e^{-(t/\sigma)^\beta} \quad (4)$$

where $\sigma > 0$ determines scale and $\alpha > 0$ and $\beta > 0$ are shape parameters. The probability density function in (4) is unimodal but may be skewed to the left or to the right. It also contains several other distributions as special cases [5, 12]. Most notably, we point out that setting $\beta = 1$ yields the Gamma distribution in (1), equating $\alpha = \beta$ yields the Weibull distribution in (2), letting $\alpha/\beta \rightarrow \infty$, the generalized Gamma distribution approaches the LogNormal distribution in (3).

These properties immediately suggest that the above results might be specific instances of a more general model. We will now prove that this is indeed the case:

Theorem 1. *The generalized Gamma distribution provides a physically plausible model of distance distributions and outbreak data in strongly-connected, undirected networks.*

Before proving this in the following subsections, we would like to stress that, in contrast to Vazquez [35] and Bauckhage *et al.* [7], our maximum entropy model does not make any assumption on the topology of the network — next to being strongly connected — through which a viral agent is spreading. Rather, it considers general properties of highly infectious processes as discussed in the introduction and resorts to the maximum entropy principle together with likelihood maximization techniques. Any aspects related to topological properties (e.g. degree distribution or clustering patterns) of individual networks are absorbed into the parameters of (4), which, as we shall see in the experimental section, is flexible enough to represent a wide range of different path length and spreading statistics.

3.1 A MAXIMUM ENTROPY APPROACH

Let us now demonstrate that the generalized Gamma distribution provides a principled model of shortest path- and outbreak statistics in networks. We argue based on Jaynes' *maximum entropy principle* [17]. It states that, subject to observations and contextual knowledge, the probability distribution that best represents the available information is the one of highest entropy. In particular, we resort to an approach by Wallis, cf. [18, chapter 11], which does not assume entropy as an a priori measure of uncertainty but uncovers it in the course of the argument.

To derive our analytical model of path length histograms of arbitrary networks, we consider the network spreading process in Fig. 1. Borrowing terminology from epidemiology, we note that, at onset time $t = 0$, most nodes in the network are *susceptible* and one node is *infected*. At time $t + 1$,

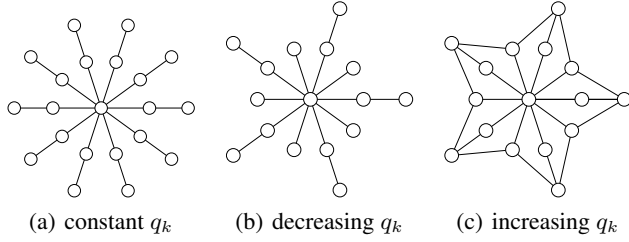


Figure 5: The probability of finding a path of length k may be constant or decrease or increase with k .

nodes that were infected at t have *recovered* yet did infect their susceptible neighbors. Highly infectious SIR cascades like this now realize a node discovery process: the number n_t of newly infected nodes at time t corresponds to the number of nodes that are at topological distance $d = t$ from the source.

Given these considerations, we observe that the discrete shortest path distribution of the entire network is nothing but the sum of all node count histograms $h_s[t]$ taken over all possible source nodes. Let K denote the length of the longest shortest path starting at a source v_s and use n_k to indicate the number of nodes that are k steps away from v_s . Then, $n = \sum_{k=0}^K n_k$ where n denotes the total number of nodes. The probability of observing a node at distance k can thus be expressed as $p_k = n_k/n$ and we have $1 = \sum_{k=0}^K p_k$. Moreover, we let q_k denote the probability that there exists a shortest path of length k so that $1 = \sum_{k=0}^K q_k$ and we emphasize that p_k and q_k will generally differ (see the didactic examples in Fig. 5). With these definitions at hand, the joint probability of observing counts n_k of infected nodes corresponds to the multinomial

$$P(n_1, \dots, n_K) = n! \prod_{k=1}^K \frac{q_k^{n_k}}{n_k!}$$

whose log-likelihood is given by

$$L = \log n! + \sum_{k=0}^K n_k \log q_k - \log n_k! \quad (5)$$

Assuming that $n_k \gg 1$, we may apply Stirling's formula $\log n_k! \approx n_k \log n_k - n_k$ to simplify (5)

$$\begin{aligned} L &\approx n \log n - n + \sum_{k=0}^K n_k (\log q_k - \log n_k + 1) \\ &= n \log n + n \sum_{k=0}^K p_k (\log q_k - (\log p_k + \log n)) \\ &= -n \sum_{k=0}^K p_k \log \frac{p_k}{q_k}. \end{aligned} \quad (6)$$

As the expression in (6) is a Kullback-Leibler divergence, our considerations so far led indeed to an entropy that needs to be maximized in order to determine the most likely values n_k^* of the n_k .

However, up until now, the quantities q_k are not defined precisely enough to allow for a solution. Also, (6) accounts

only indirectly for temporal aspects of network spreading processes as any dependency on time is hidden in the index of summation k . We address both these issues by choosing the ansatz

$$q_k = A t_k^{\alpha-1} \quad (7)$$

where A is a normalization constant and $\alpha > 0$. This choice and its significance will be justified in detail below. For now, we continue with our main argument.

Another underspecified quantity so far is the length K of the supposed longest shortest path. However, dealing with networks of finite size, we can bypass the need of having to specify K by means of introducing the following constraint

$$\sum_{k=0}^{\infty} n_k = n \quad (8)$$

into the problem of maximizing (6). Finally, to prevent degenerate solutions (e.g. instantaneous or infinite spread), we impose a constraint on the times t_k and require their moments

$$\sum_{k=0}^{\infty} \frac{n_k}{n} t_k^\beta = c \quad (9)$$

to be finite for some $\beta > 0$. Using differential forms, we now express the log-likelihood in (6) and the two constraints in (8) and (9) as

$$dL = \sum_{k=0}^{\infty} \frac{\partial L}{\partial n_k} dn_k = \sum_{k=0}^{\infty} (\log A t_k^{\alpha-1} - \log n_k) dn_k,$$

$dn = \sum_{k=0}^{\infty} dn_k$, and $dc = \sum_{k=0}^{\infty} t_k^\beta dn_k$, and consider the Lagrangian with multipliers ρ and γ

$$\mathcal{L} = \sum_{k=0}^{\infty} \left[\log \frac{A t_k^{\alpha-1}}{n_k} - \rho - \gamma t_k^\beta \right] dn_k = 0$$

in order to determine most likely infection counts n_k^* for the spreading process described above. Since at the solution the bracketed terms $[\cdot]$ must vanish identically for every dn_k , we immediately obtain

$$n_k^* = A e^{-\rho} t_k^{\alpha-1} e^{-\gamma t_k^\beta}.$$

Plugging this result back into $p_k = n_k/n$ yields a discrete probability mass function in the now exp-transformed space

$$\frac{n_k^*}{n} = \frac{t_k^{\alpha-1} e^{-\gamma t_k^\beta}}{\sum_{j=0}^{\infty} t_j^{\alpha-1} e^{-\gamma t_j^\beta}} \quad (10)$$

which explicitly relates infection counts n_k to time steps t_k . However, (10) still depends on the Lagrangian multiplier γ (now in exp-space), which is not immediately related to any available data. In order to determine γ , we assume the duration $\Delta t = t_{k+1} - t_k$ of time steps to be small. This permits the following approximation

$$\sum_{k=0}^{\infty} t_k^{\alpha-1} e^{-\gamma t_k^\beta} \Delta t \approx \int_0^{\infty} t^{\alpha-1} e^{-\gamma t^\beta} dt = \gamma^{-\frac{\alpha}{\beta}} \frac{\Gamma(\alpha/\beta)}{\beta}$$

so that

$$\frac{n_k^*}{n} = \Delta t \frac{\gamma^{\frac{\alpha}{\beta}} \beta}{\Gamma(\alpha/\beta)} t_k^{\alpha-1} e^{-\gamma t_k^\beta}.$$

Plugging this into (9), tedious but straightforward algebra yields $\gamma = \frac{\alpha}{\beta c}$ which is to say that

$$\frac{n_k^*}{n} = \Delta t \left[\frac{\beta}{\Gamma(\alpha/\beta)} \left(\frac{\alpha}{\beta c} \right)^{\frac{\alpha}{\beta}} \right] t_k^{\alpha-1} e^{-\frac{\alpha}{\beta c} t_k^\beta}. \quad (11)$$

In order to establish the final result, we now let $\Delta t \rightarrow 0$ which leads to

$$\frac{n_k^*}{n} \approx \int_{\Delta t} f(\tau) d\tau \approx \Delta t f(t) \quad (12)$$

where $t_k - \frac{\Delta t}{2} \leq t \leq t_k + \frac{\Delta t}{2}$. Direct comparison of (11) and (12) together with the substitution $\sigma = \left(\frac{\beta c}{\alpha}\right)^{1/\beta}$ finally establishes that

$$f(t) = \frac{\beta}{\sigma^\alpha} \frac{1}{\Gamma(\alpha/\beta)} t^{\alpha-1} e^{-(t/\sigma)^\beta}$$

which is indeed the generalized Gamma distribution that was introduced in (4).

3.2 EXTENSIONS TO DIFFERENT TIME SCALES

So far, our derivation above was based on properties of networked *SIR* cascades for which the infection rate i as well as the recovery rate r were both assumed to be 100%. Yet, the empirical result in Section 4 indicate that the generalized Gamma distribution also accounts for the dynamics of less infectious spreading processes where i and r are smaller. Such epidemics usually last longer as it takes more time to reach all susceptible nodes and infected nodes may remain so over extended periods. In other words, such processes can be thought of as taking place on a different time scale. Here, we briefly show that the generalized Gamma distribution can also explain spreading processes on linearly or polynomially transformed time scales.

Recall that if a random variable X is distributed according to $f(x)$, the monotonously transformed random variable $Y = h(X)$ has a probability function that is given by

$$g(y) = f(h^{-1}(y)) \cdot \left| \frac{d}{dy} h^{-1}(y) \right|.$$

Now, if t is generalized Gamma distributed and $\tau = ct$ is a linearly transformed version of t , then

$$t = \frac{\tau}{c} \quad \text{and} \quad \frac{dt}{d\tau} = \frac{1}{c}$$

so that τ is distributed according to

$$\begin{aligned} g(\tau) &= \frac{\beta}{\sigma^\alpha} \frac{1}{\Gamma(\alpha/\beta)} \left(\frac{\tau}{c} \right)^{\alpha-1} e^{-(\tau/c\sigma)^\beta} \cdot \frac{1}{c} \\ &= \frac{\beta}{\sigma'^\alpha} \frac{1}{\Gamma(\alpha'/\beta')} \tau^{\alpha'-1} e^{-(\tau/\sigma')^\beta} \end{aligned}$$

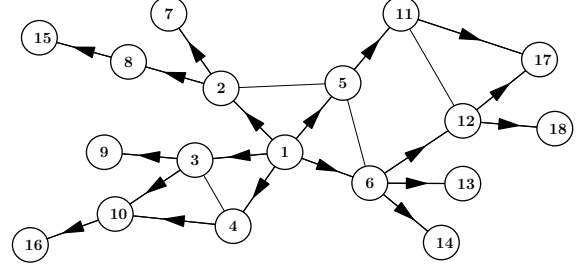


Figure 6: Causal graph of the process in Fig. 1. The adjacency matrix of a directed acyclic graph with a single source node can be brought into strictly upper triangular form and is thus nilpotent.

which is a generalized Gamma distribution with scale parameter $\sigma' = c\sigma$.

By the same token, if t is generalized Gamma distributed and $\tau = t^c$ is a polynomially transformed version of t , then

$$t = \tau^{\frac{1}{c}} \quad \text{and} \quad \frac{dt}{d\tau} = \frac{1}{c} \tau^{\frac{1}{c}-1}$$

so that τ is distributed according to

$$\begin{aligned} g(\tau) &= \frac{\beta}{\sigma^\alpha} \frac{1}{\Gamma(\alpha/\beta)} \left(\tau^{\frac{1}{c}} \right)^{\alpha-1} e^{-(\tau^{1/c}/\sigma)^\beta} \cdot \frac{1}{c} \tau^{\frac{1}{c}-1} \\ &= \frac{\beta' c}{\sigma'^{\alpha'}} \frac{1}{\Gamma(\alpha'/\beta')} \tau^{\alpha'-1} e^{-(\tau^{\beta'}/\sigma'^{\beta'})} \end{aligned}$$

which is a generalized Gamma distribution with parameters $\sigma' = \sigma^c$, $\alpha' = \frac{\alpha}{c}$, and $\beta' = \frac{\beta}{c}$.

3.3 JUSTIFYING THE POLYNOMIAL ANSATZ (7)

While the constraints in (8) and (9) are arguably intuitive, the ansatz in (7) merits further elaboration. Note that *causal graphs* as in Fig. 6 indicate possible transmission pathways of an epidemic. In general they may be arbitrarily complex but, for the type of spreading process studied here, they are necessarily directed and acyclic. Now, in a directed, acyclic graph, the number N_k of shortest paths of lengths k starting from a source node v_s may indeed grow exponentially for a while (for instance in a tree) but the finite size of the graph causes N_k to drop to zero once k exceeds the length K of the longest shortest path; there are no shortest paths longer than K . Because of this finite size effect, a polynomial upper bound always exists for N_k , $k \leq K$.

More formally, consider a network of n nodes. If v_s is the source node of an epidemic on this network and \mathbf{A} is the adjacency matrix¹ of the corresponding causal graph then $(\mathbf{A}^k)_{s_j}$ denotes number of ways the epidemic agent can reach v_j from v_s in k steps and $q_k \propto \sum_j (\mathbf{A}^k)_{s_j}$. For causal

¹ $A_{ij} = 1$ if nodes v_i infects v_j , and $A_{ij} = 0$ otherwise.

graphs, \mathbf{A} is strictly upper triangular and therefore *nilpotent*. That is, $\exists K \leq n : \mathbf{A}^k = \mathbf{0} \ \forall k > K$. Hence, $\rho(\mathbf{A}) < 1$ which is to say $\exists u > 0 : \|\mathbf{A}^k\|_F < u \ \forall k$ and therefore $0 \leq (\mathbf{A}^k)_{sj} \leq \|\mathbf{A}^k\|_F < u$. Accordingly, $\sum_j (\mathbf{A}^k)_{sj} \in O(k^{\alpha-1})$ for some $\alpha \geq 1$. Setting $t_k = \epsilon k$ where $\epsilon \leq 1$ yields $q_k \in O(t_k^{\alpha-1})$ which justifies (7).

Put in simple terms, it is sufficient to model the probability q_k of observing an epidemic path of length k as a polynomial in t rather than, say, an exponential function.

The fact that the parameter α reflects aspects of network topology is easily seen from the examples in Fig. 5. Assuming the central node to be the source node of an epidemic the figure shows that q_k may be constant ($\alpha = 1$), decreasing ($\alpha < 1$), or increasing ($\alpha > 1$) with k .

4 EMPIRICAL SUPPORT

We now support our theoretical results with empirical evidence. First, we present results on distance distributions of synthesized networks. Then, we report on experiments with a large number of spreading processes on synthetic graphs and, finally, we discuss results obtained for large, real-world networks.

Throughout, we fit continuous distributions to discrete histograms. That is, we apply functions $f(t; \theta)$ to represent counts n_0, \dots, n_K which are grouped into K distinct intervals $(t_0, t_1], (t_1, t_2], \dots, (t_{K-1}, t_\infty)$. For this setting, it is advantageous to use multinomial likelihood estimation based on reweighted least squares in order to determine optimal model parameters θ^* [19]. For a recent detailed exposition of this robust technique, we refer to [6]. For the fitted models, we report quantitative goodness-of-fit results in terms of the Hellinger distance

$H(h[t], f[t]) = \frac{1}{2} \sqrt{\sum_t \left(\sqrt{h[t]} - \sqrt{f[t]} \right)^2}$ between discrete empirical data $h[t]$ and a discretized model $f[t]$ where

$$f[t] = \begin{cases} F(t + \frac{1}{2}) & \text{if } t = 0 \\ F(t + \frac{1}{2}) - F(t - \frac{1}{2}) & \text{if } 0 < t < K \\ 1 - F(t + \frac{1}{2}) & \text{if } t = K \end{cases}$$

and $F(\cdot)$ is the corresponding cumulative density function. We note that the Hellinger distance is bound as $0 \leq H \leq 1$.

Synthetic Networks. We created different Erdős-Rényi (ER), Barabási-Albert (BA), power law (PL), and Log-Normal (LN) graphs of $n \in \{5,000, 10,000\}$ nodes. ER graphs are a staple of graph theory and merit investigation. To create ER graphs, we used edge probability parameters $\pi \in \{0.005, 0.0075, 0.01\}$. BA and PL graphs represent networks that result from preferential attachment processes and are frequently observed in biological, social, and technical contexts. To create BA graphs, we considered attachment parameters $m \in \{1, 2, 3\}$ and exponents

Table 1: Goodness of Fit (avg. Hellinger distances) for shortest path histograms of synthetic networks

network	parameters	f_{WB}	f_{GA}	f_{LN}	f_{GG}
ER	$\pi = 0.0050$	0.058	0.170	0.227	0.051
	$\pi = 0.0075$	0.046	0.164	0.205	0.041
BA	$m = 1$	0.039	0.066	0.135	0.011
	$m = 2$	0.017	0.125	0.170	0.015
	$m = 3$	0.015	0.128	0.171	0.015
PL	$\gamma = 2.1$	0.154	0.042	0.040	0.030
	$\gamma = 2.3$	0.132	0.032	0.046	0.024
	$\gamma = 2.5$	0.123	0.037	0.064	0.028
	$\gamma = 2.7$	0.101	0.044	0.089	0.028
	$\gamma = 2.9$	0.081	0.050	0.108	0.026
	$\gamma = 3.1$	0.070	0.093	0.137	0.051
LN	$\mu = 1, \xi = 0.75$	0.075	0.093	0.149	0.037
	$\mu = 1, \xi = 1.25$	0.082	0.067	0.113	0.029
	$\mu = 2, \xi = 0.75$	0.073	0.092	0.145	0.036
	$\mu = 2, \xi = 1.25$	0.079	0.062	0.102	0.026

of the vertex degree distributions of the PL graphs were drawn from $\gamma \in \{2.1, 2.2, \dots, 3.2\}$. LN graphs show log-normally distributed vertex degrees and reportedly characterize link structures within sub-communities on the web [30]. To synthesize LN graphs, parameters were chosen from $\mu \in \{1, 1.5, \dots, 3\}$ and $\xi \in \{0.25, 0.5, 0.75, 1\}$. For each parametrization, we created 100 instances.

Table 1 summarizes average goodness of fit results for graphs of $n = 10,000$ nodes and different topologies (for lack of space, we omit results for some of the parametrizations considered in our experiments). We observe that (i) in agreement with Bauchhage *et al.* [7], the Weibull distribution provides a well fitting model for the distance distribution in ER graphs; it outperforms the Gamma and the Log-Normal distribution; (ii) in agreement with Vazquez [35], the Gamma distribution provides a well fitting model for PL graphs where $2 < \gamma < 3$; (iii) for PL graphs where $\gamma \lesssim 2.2$, the LogNormal fits well, too; (iv) for PL graphs where $\gamma \geq 3$, the Weibull fits better than the Gamma or the LogNormal; in this context, we note that BA graphs are power law graphs for which $\gamma = 3$ [3]; (v) in any case, the generalized Gamma distribution provides the best fits in all cases while still being physically plausible.

Indeed, the latter is not surprising as the densities in (1)-(3) are functions of two parameters whereas the generalized gamma in (4) depends on three parameters and therefore offers greater flexibility in statistical model fitting. However, as proven above, the generalized gamma also follows from first principle and provides accurate fits across a wide variety of underlying network topologies, while the Gamma and the Weibull distribution apply to particular types of networks only. In turn and probably most important, the traditional reliance of investigating several distributions can be eliminated. Moreover, as we will demonstrate below, even without regularization, which is an interesting avenue for

future work, the parameters of the generalized Gamma indeed allow one to distinguish different graph classes.

Spreading Processes. Given the synthetic networks created above, we simulated *SIR* spreading processes where the infection rate varied in $i \in \{0.5, 0.6, \dots, 0.9\}$ and the recovery rate was chosen from $r \in \{0.5, 0.6, \dots, 0.9\}$. For each network and each choice of i and r , we created 10 epidemics starting at randomly selected source nodes v_s and fitted the generalized Gamma to the resulting outbreak data.

Table 2 shows exemplary results obtained for PL graphs of 10,000 nodes; rows correspond to different power law exponents γ and columns indicate different choices of pairs (i, r) . Each panel plots the outbreak data of all the corresponding epidemics (grey dots), the corresponding empirical average taken over the individual outbreak distributions (black dots), as well as a generalized Gamma fit to these averages (blue curves). Visual inspection of these results suggests that the generalized Gamma distribution accounts very well for average outbreak dynamics in power law graphs. Though not shown in the table, this behavior was also observed for individual epidemics as well as for epidemics on other networks, hence, supporting our theoretical justification provided in Sec. 3.2.

Real-World Networks. The KONECT network collection [23] provides a comprehensive set of large scale, real-world network data freely available for research. Networks contained in this collection comprise (online) social networks where edges indicate social contacts or friendship relations, natural networks such as power grids or connections between airports, and bipartite networks such as typically found in the context of recommender systems. The sizes of these networks vary between $O(10,000)$ to $O(1,000,000)$ nodes and they show different node degree distributions and clustering coefficients. For further details, we refer to <http://konect.uni-koblenz.de/>.

Tables 3 through 5 summarize goodness-of-fit results obtained from fitting the models in (1), (2), (3), and (4) to hop count distributions of social, natural, and bipartite networks respectively. Again in agreement with the theoretical prediction in [35], we observe that the Gamma distribution provides accurate fits to path length distributions in social networks which are often reported to be power law networks with power law exponents $2 < \gamma < 3$. For the case of natural and bipartite networks, we find the LogNormal distribution to provide better fits than the Gamma or the Weibull distribution. We emphasize that this is an empirical finding which, to our knowledge, has not yet been justified theoretically. In this sense, the work presented in this paper can be seen as the first such justification because the LogNormal is obtained a limiting case of the generalized Gamma distribution which, as shown in Sec. 3.1, provides a physically plausible model of distance distributions in networks. In fact, just as in the previous subsections, the

Table 3: Goodness of Fit (Hellinger distances) for shortest path histograms of social networks

network	f_{WB}	f_{GA}	f_{LN}	f_{GG}
advogato	0.110	0.014	0.056	0.012
arenas email	0.044	0.036	0.074	0.008
arenas pgp	0.100	0.022	0.057	0.013
ca AstroPh	0.157	0.021	0.047	0.021
ca cit HepPh	0.133	0.023	0.065	0.015
ca cit HepTh	0.089	0.016	0.026	0.010
catster	0.101	0.023	0.032	0.016
cfinder google	0.076	0.021	0.023	0.032
cit HepPh	0.178	0.037	0.065	0.032
cit HepTh	0.135	0.018	0.051	0.016
dblp cite	0.078	0.042	0.077	0.012
dogster	0.215	0.036	0.048	0.026
elec	0.046	0.057	0.096	0.020
email EuAll	0.363	0.331	0.116	0.232
enron	0.122	0.046	0.075	0.023
facebook wosn links	0.186	0.022	0.037	0.018
facebook wosn wall	0.172	0.025	0.048	0.021
filmtipset friend	0.140	0.024	0.052	0.017
gottron net all	0.075	0.038	0.070	0.029
gottron net core	0.049	0.024	0.060	0.006
hep th citations	0.122	0.011	0.036	0.009
loc brightkite edges	0.193	0.027	0.035	0.059
munmun digg reply	0.170	0.028	0.054	0.023
munmun twitter social	0.132	0.089	0.079	0.071
collaboration	0.137	0.097	0.074	0.045
ucsocial	0.084	0.012	0.056	0.008
petster carnivore	0.120	0.116	0.119	0.117
petster friendships cat	0.109	0.023	0.032	0.027
petster friendships dog	0.206	0.036	0.048	0.026
petster friendships hamster	0.167	0.083	0.049	0.060
petster hamster	0.081	0.011	0.033	0.007
sap	0.142	0.063	0.090	0.052
slashdot threads	0.267	0.082	0.055	0.102
slashdot zoo	0.192	0.026	0.052	0.032
wikiconflict	0.134	0.014	0.055	0.014
wikisigned k2	0.268	0.166	0.070	0.136
wikisigned nontext	0.291	0.086	0.058	0.066
avg.	0.146	0.050	0.059	0.039

Table 4: Goodness of Fit (Hellinger distances) for shortest path histograms of natural networks

network	f_{WB}	f_{GA}	f_{LN}	f_{GG}
arenas meta	0.090	0.036	0.025	0.029
as caida20071105	0.277	0.160	0.050	0.113
as20000102	0.065	0.016	0.054	0.005
dbpedia similar	0.685	0.686	0.082	0.018
eat	0.012	0.075	0.115	0.003
lasagne frenchbook	0.017	0.001	0.058	0.003
openflights	0.139	0.025	0.040	0.022
powergrid	0.745	0.745	0.150	0.016
usairport	0.053	0.010	0.040	0.007
sociopatterns infectious	0.030	0.026	0.053	0.012
topology	0.130	0.021	0.055	0.019
wordnet words	0.192	0.031	0.054	0.022
wordnet	0.133	0.188	0.214	0.131
avg.	0.198	0.155	0.076	0.031

Table 2: Outbreak data obtained from spreading processes in power law networks of 10,000 nodes

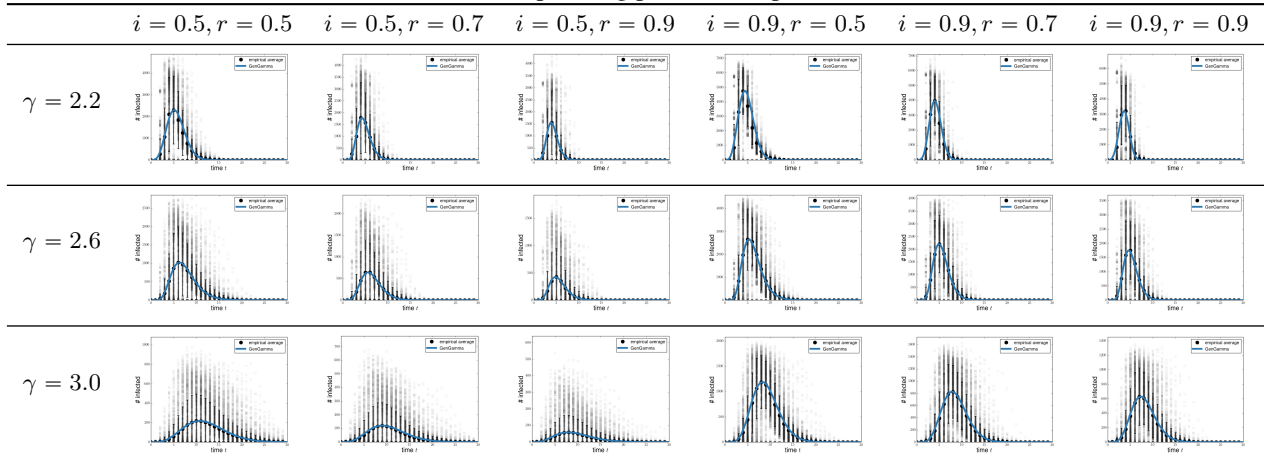


Table 5: Goodness of Fit (Hellinger distances) for shortest path histograms of bipartite networks

network	f_{WB}	f_{GA}	f_{LN}	f_{GG}
adjnoun	0.028	0.037	0.065	0.012
bx	0.264	0.096	0.090	0.130
dbpedia occupation	0.165	0.103	0.113	0.101
dbpedia producer	0.734	0.734	0.152	0.156
dbpedia starring	0.721	0.721	0.034	0.032
dbpedia writer	0.754	0.754	0.096	0.072
epinions	0.209	0.036	0.041	0.026
escorts	0.097	0.048	0.076	0.031
filmtipset comment	0.060	0.049	0.089	0.007
github	0.186	0.078	0.082	0.078
gottron reuters	0.128	0.112	0.137	0.106
movielens 10m ti	0.187	0.082	0.101	0.074
movielens 10m ui	0.036	0.083	0.116	0.031
movielens 10m ut	0.199	0.146	0.159	0.144
movielens 1m	0.043	0.005	0.040	0.007
ucforum	0.047	0.050	0.080	0.030
pics ut	0.268	0.164	0.166	0.183
prosper support	0.230	0.259	0.232	0.208
youtube groupmemberships	0.192	0.115	0.119	0.115
avg.	0.239	0.193	0.105	0.081

generalized Gamma distribution is again found to provide the best overall fits to the data considered here. Qualitative examples of this behavior are shown in Fig. 7.

We also evaluated how the different distributions perform in predicting the average shortest path length and compared empirical means to the means of fitted models. For the Weibull, the mean is given by $\lambda\Gamma(1 + 1/\kappa)$, the mean of the Gamma is $\eta\theta$, that of the LogNormal is $\exp(\mu - \xi^2/2)$, and for the generalized Gamma we have $\mathbb{E}\{t\} = \sigma \frac{\Gamma((\alpha+1)/\beta)}{\Gamma(\alpha/\beta)}$. Using these formulas, we investigated predicted average shortest path lengths versus empirically determined ones for the networks in the KONECT collection. The results are summarized in Tab. 6, which lists mean squared square errors for the data in the figure. They suggests that w.r.t. predicting average path lengths, the Weibull performs worse

Table 6: Mean squared errors for predicted average shortest path lengths versus empirically determined ones for the networks in the KONECT collection.

	f_{WB}	f_{GA}	f_{LN}	f_{GG}
bipartite	1.665	1.382	0.731	0.414
natural	0.216	0.479	0.862	0.093
social	0.474	0.219	0.648	0.220
overall	1.745	1.479	1.303	0.478

than the Gamma which performs worse than the LogNormal which is outperformed by the generalized Gamma.

Distinguishing between Different Graph Classes. An interesting consequence of fitting the distance distribution using the three-parameter generalized Gamma is that it provides a non-linear mapping of path length data into three dimensions. This allows for visual analytics of the behavior of different graph topologies w.r.t. distance distributions. Fig. 8 shows exemplary distance distributions in terms 3D coordinates (σ, α, β) that result from fitting generalized Gamma distributions. Looking at the Figure, it appears that distance distributions obtained from different network topologies cluster together or are confined to certain regions in this parameter space. These preliminary observations are arguably the most interesting finding in this paper as they suggest that the idea of characterizing networks in terms of continuous models of shortest path distributions can inform approaches to the problem of network inference from outbreak data. Investigating these results more deeply provides an interesting avenue for future work.

5 CONCLUSIONS

We considered the problem of parameterizing the distance distribution and epidemic outbreak data of strongly-connected, undirected networks. Invoking the maxi-

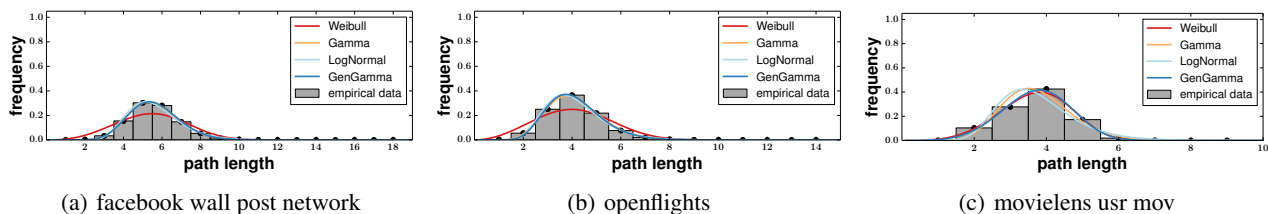


Figure 7: Qualitative examples of shortest path distributions on real-world networks. Path length distributions of social and natural networks are well accounted for by the Gamma distribution (a+b) whereas the Weibull provides better fits for bipartite networks that occur in recommender settings (c). In each case, however, the generalized Gamma fits best.

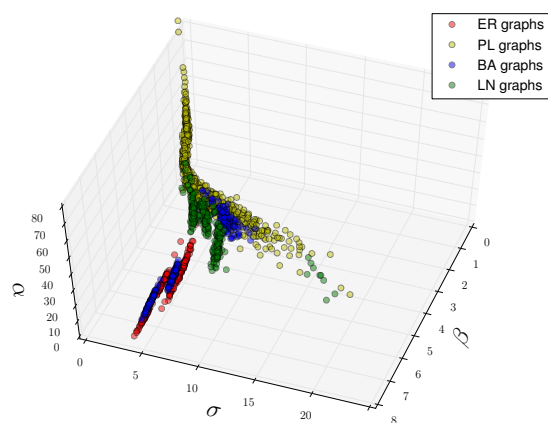
mum entropy principle, we showed that the generalized Gamma distribution provides a physically plausible, three-parameter distribution for these data, independent of the topology of the underlying networks. This result generalizes earlier models [7, 35] and explains recent empirical observations made w.r.t. twitter retweet networks [8]. Empirical tests confirmed our theoretical prediction and revealed that the generalized Gamma distribution accounts well for distance distributions of synthesized Erdős-Rényi, Barabási-Albert, power law, and LogNormal graphs as well as for real-world network in the KONECT collection [23]. Finally, we illustrated that the parameters of the generalized Gamma provide striking structural regularities in the resulting low-dimensional network representations.

Our results suggest several attractive avenues for future research. First of all, one should relate the shape and scale parameters of the generalized Gamma distribution to physical properties or well established features of networks. Second, one should use our theoretical results to devised informed sampling schemes for the problem of computing shortest paths (and their histograms) for large real-world networks. Finally, the results in Fig. 8 suggest a nearest-neighbour approach to network inference from outbreak data. Newly observed epidemic processes are matched to a large data base of 3D representations of outbreak data, for which the network is known; at least this provides helpful prior information for network inference approaches such as [32, 22].

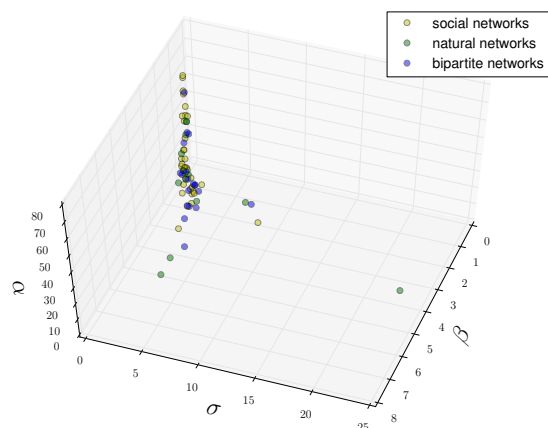
Acknowledgments. The authors would like to thank the anonymous reviewers for their feedback. The work was partly supported by the DFG Collaborative Research Center SFB 876 project A6.

References

- [1] D. Acemoglu, A. Ozdaglar, and M.E. Yildiz. Diffusion of Innovations in Social Networks. In *Proc. Int. Conf. on Decision and Control*. IEEE, 2011.
- [2] E. Adar and A. Adamic. Tracking Information Epidemics in Blogspace. In *Proc. Int. Conf. on Web Intelligence*. IEEE/WIC/ACM, 2005.
- [3] A.L. Barabasi and R. Albert. Emergence of Scaling



(a) synthetic networks



(b) real-world networks

Figure 8: 3D embedding of shortest path histograms from different networks. Each point (σ, α, β) represents a path length distribution in terms of the parameters of the best fitting generalized Gamma model. Different classes of graphs appear to be confined to specific regions.

in Random Networks. *Science*, 286(5439):509–512, 1999.

- [4] M. Barthelemy, A. Barrat, R. Pastor-Satorras, and A. Vespignani. Velocity and Hierarchical Spread of

- Epidemic Outbreaks in Scale-free Networks. *Physical Review Letters*, 92(17):178701, 2004.
- [5] C. Bauckhage. Computing the Kullback-Leibler Divergence between two Generalized Gamma Distributions. *arXiv:1401.6853 [cs.IT]*, 2014.
- [6] C. Bauckhage and K. Kersting. Strong Regularities in Growth and Decline of Popularity of Social Media Services. *arXiv:1406.6529 [cs.SI]*, 2014.
- [7] C. Bauckhage, K. Kersting, and B. Rastegarpanah. The Weibull as a Model of Shortest Path Distributions in Random Networks. In *Proc. Int. Workshop on Mining and Learning with Graphs*, 2013.
- [8] D.R. Bild, Y. Liu, R.P. Dick, Z. Morley Mao, and D.S. Wallach. Aggregate Characterization of User Behavior in Twitter and Analysis of the Retweet Graph. *ACM Trans. on Internet Technology*, 15(1):1–24, 2015.
- [9] V.D. Blondel, J.L. Guillaume, J.M. Hendrickx, and R.M. Jungers. Distance Distribution in Random Graphs and Application to Network Exploration. *Physical Review E*, 76(6):066101, 2007.
- [10] C. Budak, D. Agrawal, and A. El Abbadi. Limiting the Spread of Misinformation in Social Networks. In *Proc. WWW*. ACM, 2010.
- [11] R. Cohen and S. Havlin. *Complex Networks*. Cambridge University Press, 2010.
- [12] G.E. Crooks. The Amoroso Distribution. *arXiv:1005.3274 [math.ST]*, 2010.
- [13] L. de Haan and A. Ferreira. *Extreme Value Theory*. Springer, 2006.
- [14] A. Fronczak, P. Fronczak, and J.A. Holyst. Average Path Length in Random Networks. *Physical Review E*, 70(5):056110, 2004.
- [15] M. Gomez-Rodriguez, J. Leskovec, and B. Schölkopf. Structure and Dynamics of Information Pathways in Online Media. In *Proc. WSDM*. ACM, 2013.
- [16] J.L. Iribarren and E. Moro. Impact of Human Activity Patterns on the Dynamics of Information Diffusion. *Physical Review Letters*, 103(3):038702, 2009.
- [17] E.T. Jaynes. Information Theory and Statistical Mechanics. *Physical Review*, 106:620–630, 1957.
- [18] E.T. Jaynes. *Probability Theory: The Logic of Science*. Cambridge University Press, 2003.
- [19] R.I. Jennrich and R.H. Moore. Maximum Likelihood Estimation by Means of Nonlinear Least Squares. In *Proc. of the Statistical Computing Section*. American Statistical Association, 1975.
- [20] M.J. Keeling and K.T.D. Eames. Networks and Epidemic Models. *J. Royal Society Interface*, 2(4):295–307, 2005.
- [21] D. Kempe, J. Kleinberg, and E. Tardos. Maximizing the Spread of Influence through A Social Network. In *Proc. KDD*. ACM, 2003.
- [22] A. Kumar, D. Sheldon, and B. Srivastava. Collective diffusion over networks: Models and inference. In *Proc. UAI*, 2013.
- [23] J. Kunegis. KONECT: the Koblenz Network Collection. In *Proc. WWW*. ACM, 2013.
- [24] J. Leskovec, L.A. Adamic, and B.A. Huberman. The Dynamics of Viral Marketing. *ACM Trans. Web*, 1(1):5, 2007.
- [25] J. Leskovec, L. Backstrom, and J. Kleinberg. Meme-tracking and the Dynamics of the News Cycle. In *Proc. KDD*. ACM, 2009.
- [26] J. Leskovec, M. McGlohon, C. Faloutsos, N. Glance, and M. Hurst. Patterns of Cascading Behavior in Large Blog Graphs. In *Proc. Int. Conf on Data Mining*. SIAM, 2007.
- [27] A.L. Lloyd and R.M. May. How Viruses Spread Among Computers and People. *Science*, 292(5520):1316–1317, 2001.
- [28] M.E.J. Newman. The Spread of Epidemic Diseases on Networks. *Physical Review E*, 66(1):016128, 2002.
- [29] R. Pastor-Satorras and A. Vespignani. Epidemic Spreading in Scale-Free Networks. *Physical Review Letters*, 86(14):3200–3203, 2001.
- [30] D.M. Pennock, G.W. Flake, S. Lawrence, E.J. Glover, and C.L. Gilles. Winners Don’t Take All: Characterizing the Competition for Links on the Web. *PNAS*, 99(8):5207–5211, 2002.
- [31] H. Rinne. *The Weibull Distribution*. Chapman & Hall / CRC, 2008.
- [32] D. Sheldon, B.N. Dilkina, A.N. Elmachtoub, R. Finseth, A. Sabharwal, J. Conrad, C.P. Gomes, D.B. Shmoys, W. Allen, O. Amundsen, and W. Vaughan. Maximizing the spread of cascades using network design. In *In Proc. UAI*, pages 517–526, 2010.
- [33] E.W. Stacy. A Generalization of the Gamma Distribution. *The Annals of Mathematical Statistics*, 33(3):1187–1192, 1962.
- [34] A. Ukkonen. Indirect Estimation of Shortest Path Distributions with Small-World Experiments. In *Proc. Advances in Intelligent Data Analysis*, 2014.
- [35] A. Vazquez. Polynomial Growth in Branching Processes with Diverging Reproduction Number. *Physical Review Letters*, 96(3):038702, 2006.
- [36] J. Yang and J. Leskovec. Patterns of Temporal Variation in Online Media. In *Proc. WSDM*. ACM, 2011.